An anchoring system for supporting platforms for wind energy devices

Sivakumar, Vinayagamoorthy; Fanning, Joseph; Gavin, Ken; Tripathy, Snehasis; Bradshaw, Aaron; Murray, Edward J.; Black, Jonathan; Donohue, Shane

DOI
10.1680/jgeen.22.00245

Publication date
2023

Document Version
Final published version

Published in
Proceedings of the Institution of Civil Engineers: Geotechnical Engineering

Cite this article
Sivakumar V, Fanning J, Gavin K *et al.*
An anchoring system for supporting platforms for wind energy devices.
Proceedings of the Institution of Civil Engineers – Geotechnical Engineering,
https://doi.org/10.1680/jgeen.22.00245

Research Article
Paper 2200245
Received 12/12/2022;
Accepted 04/07/2023;
First published online 25/07/2023

Geotechnical Engineering

An anchoring system for supporting platforms for wind energy devices

Vinayagamoorthy Sivakumar MSc, MIC, DIC, PhD, CEng, FICE, DSc
Reader, Queen's University Belfast, Belfast, UK (corresponding author: v.sivakumar@qub.ac.uk)

Joseph Fanning MEng, PhD
Senior Geotechnical Engineer, Queen's University Belfast, Belfast, UK

Ken Gavin MEng, PhD, CEng
Professor of Subsurface Engineering, Faculty of Civil Engineering and Geosciences, Delft University of Technology, Delft, the Netherlands

Snehasis Tripathy MTech, PhD
Professor, School of Engineering, Cardiff University, Cardiff, UK

Aaron Bradshaw PhD
Professor, Civil and Environmental Engineering, University of Rhode Island, Kingston, RI, USA

Edward J. Murray BEng, PhD, CEng
Consultant, Murray Rix Limited, Stoke Golding, UK

Jonathan Black BEng, PhD
Lecturer, Queen's University Belfast, Belfast, UK

Shane Donohue MEng, PhD
Associate Professor, University College of Dublin, Dublin, Ireland

This paper presents data from an initial development stage of an 'umbrella anchor' concept. The anchor can be pushed into a sand deposit in a folded arrangement to reduce installation loads. When a pull-out load is applied to the mooring line, the anchor deploys to create a large embedded plate anchor. Physical modelling was carried out in a saturated sand bed with the anchor installed at depths of up to 1.6 m and loaded vertically. During installation, liquefaction was generated at the tip of the anchor to reduce the penetration resistance. This enabled the anchor to be installed quickly and accurately to a target depth. The anchor could provide pull-out resistances comparable to an anchor that has been wished-in-place at similar depths. The observed behaviour provided encouraging preliminary results and suggests that, with further development and analysis, the concept could potentially be used for commercial applications.

Keywords: anchors & anchorages/buried structures/granular materials/laboratory tests/model tests

Notation

D	projected or equivalent dimension (Figure 4)
D_1	equivalent dimension to the width (Figure 4)
D_2	equivalent diameter of a circular plate (Figure 4)
D_{10}	particle size passing 10% of particles
D_{30}	particle size passing 30% of particles
D_{60}	particle size passing 60% of particles
H	anchor depth
N_q	breakout factors
N_{qf1}	breakout factors for $H/D = 1.0$
N_{qf10}	breakout factors for $H/D = 10.0$
N_γ	normalised capacity factor
q_u	pull-out forced divided by the anchor area
W	space between fully opened wings (Figure 4)
γ'	effective unit weight
Φ'	internal friction angle

1. Introduction

Many existing offshore turbines are constructed in water depths between 20 and 60 m (Gavin *et al.*, 2011). As the oil and gas industry moves into areas of deeper water, diverse anchor concepts are being developed to support floating wind turbine platforms (Randolph *et al.*, 2011). The choice of anchoring system is determined by various factors: size and type of floating structure, mooring system, seabed conditions and the design life. The anchors commonly known in the industry are anchor piles, suction caissons, drag anchors, torpedo anchors, plate anchors and helical anchors.

Pile anchors are installed by vibration, driving or drilling and grouting in place. However, the use of these anchors is expensive due to the equipment necessary to install them in deep water. Torpedo anchors behave in the same way as pile anchors. These anchors can be dropped from a known height above the seabed, and they can penetrate the seabed under their self-weight. The final embedment depth and the pull-out capacity of these anchors are difficult to predict but can be determined after installation. However, such an installation process is not feasible in granular deposits or ground with complex geology (Frankenmolen *et al.*, 2017: Richardson, 2008). Suction caissons are the most used anchoring systems for various applications both in shallow and deep-water installations, owing to their ability to resist horizontal and vertical loading and their simple installation and removal processes (Houlsby and Byrne, 2005). Caissons were used as the anchoring system for the world's first grid connected floating turbines for the Hywind project in Scotland. Helical anchors are feasible in sand deposits for providing pull-out capacity (Byrne and Houlsby, 2015; Ullah *et al.*, 2023).

Plate anchors consist of a fluke, which provides the main bearing surface, and a central shank, which connects the fluke to the mooring line. Plate anchors are installed by dragging them into the seabed. To drag an anchor to a target depth, it may have to be dragged large distances, which will increase the site investigation costs and installation time. These anchors provide an efficient option for foundations in terms of their potential pull-out capacity relative to their self-weight. Experimental and numerical investigations showed that the pull-out capacity in both sand and

clay varied with anchor shape, soil strength and the depth below the seabed, normalised by anchor width (Aubeny, 2019; Das and Seeley, 1975; Giampa *et al*., 2019; Jalilvand *et al*., 2022; Lai *et al*., 2020; Liu *et al*., 2010, 2012; Meyerhof and Adams, 1968; Neubecker and Randolph, 1996; O'Neill *et al*., 2003; Roy *et al*., 2021a, 2021b; Sahoo and Ganesh, 2018; Thorne, 1998; Vesic, 1971: Yu *et al*., 2015: Zhuang *et al*., 2022). Novel concepts such as the suction embedded plate anchor (Zook and Keith, 2009), OMNI-Max anchor (Kim and Hossain, 2017), multiline ring anchor (Lee *et al*., 2021, Lee and Aubeny, 2020), fish anchor (Chang *et al*., 2019, Hossain *et al*., 2023) and dynamically embedded plate anchor (O'Loughlin *et al*., 2014) have been developed in recent years. Constitutive parameters can change with stress level. Therefore, carrying out investigations under 1***g*** conditions may not be fully representative of the in situ conditions. On that note, there have been notable investigations carried out on plate anchors under elevated acceleration (centrifuge modelling by Giampa *et al*. (2017) and Roy *et al*. (2021a, 2021b)).

In the current investigation, a concept for an umbrella anchor was investigated. Existing information on an umbrella anchor is limited, except a single investigation was carried at the U.S. Naval Civil Engineering Laboratory (Smith, 1963). The system was then called a 'pile anchor' and it was designed for conditions in which the installation of standard piles of sufficient size was impractical or too expensive and the dragging of anchors, if needed, was limited by space or safety concerns. The umbrella anchor system proposed in this paper is self-installing (with the aid of vibration and liquefaction), thus reducing cost and installation time. It is the intention of the present research to see if the proposed umbrella anchor mechanism can create a large bearing area upon pull-out and therefore enhance the load-carrying capacity.

2. Anchor concept

The anchor is designed in the shape of an inverted pyramid (Figure 1). It has four wings that remain in an inverted pyramid shape during installation and then open up when the anchor is pulled vertically upwards, to create a large plate area. The outer edges of the wings are tapered to facilitate the penetration of the wings into the surrounding soil upon pull-out. To enable the four wings to rotate, each was connected to the central cone through pin joints, as shown in Figures 1 and 2. When the anchor wings are fully deployed, small protrusions on the central cone provide support to the wings, as shown in Figure 2. It is acknowledged that in the present proposed design, there will be significant bending moments on the wings, shear stresses on the pins and bearing stresses on the support. These aspects will be discussed in more detail later in this paper. A 'follower', shown in Figure 3, was designed to allow the anchor to be pushed into the soil bed. To reduce the forces required for the anchor to be installed, localised liquefaction was generated in the soil. This was achieved by applying a water jet at a pressure of about 50 kPa at the tip of the anchor. In addition, a vibrating hammer (capacity 8 J and 50 Hz frequency) was attached at the top of the follower to accelerate the installation process. Following the completion of installation and the removal of the follower, a pull-out load was applied to the mooring line.

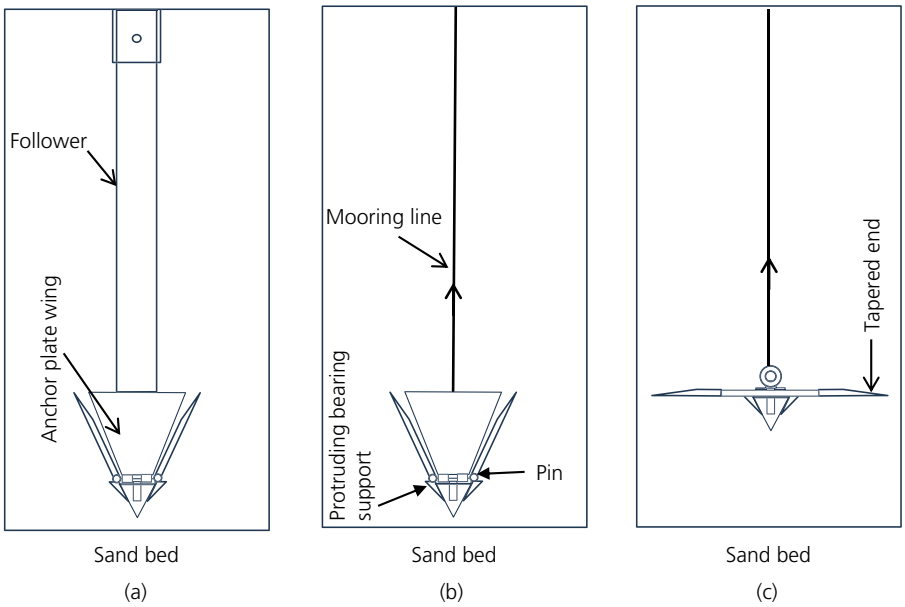

Figure 1. Umbrella anchor installation: (a) the anchor is pushed into place using the follower with the mooring line through the centre of the follower; (b) the follower is removed and pull-out force is applied to the mooring line; (c) the anchor moves vertically and opens to create an embedded plate anchor

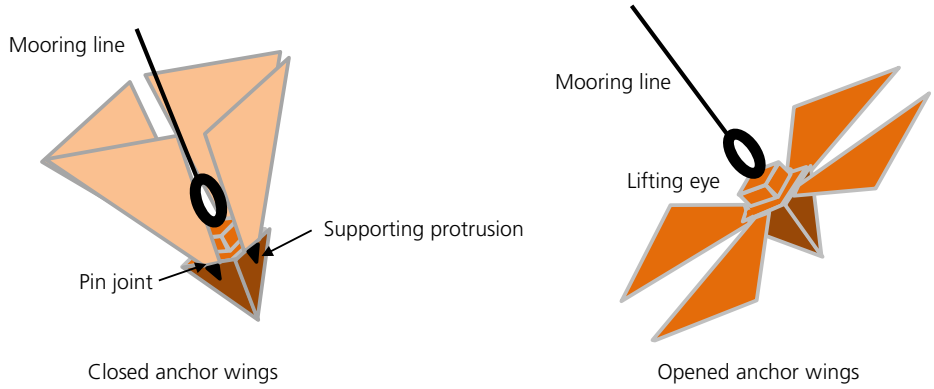

Figure 2. Umbrella anchor

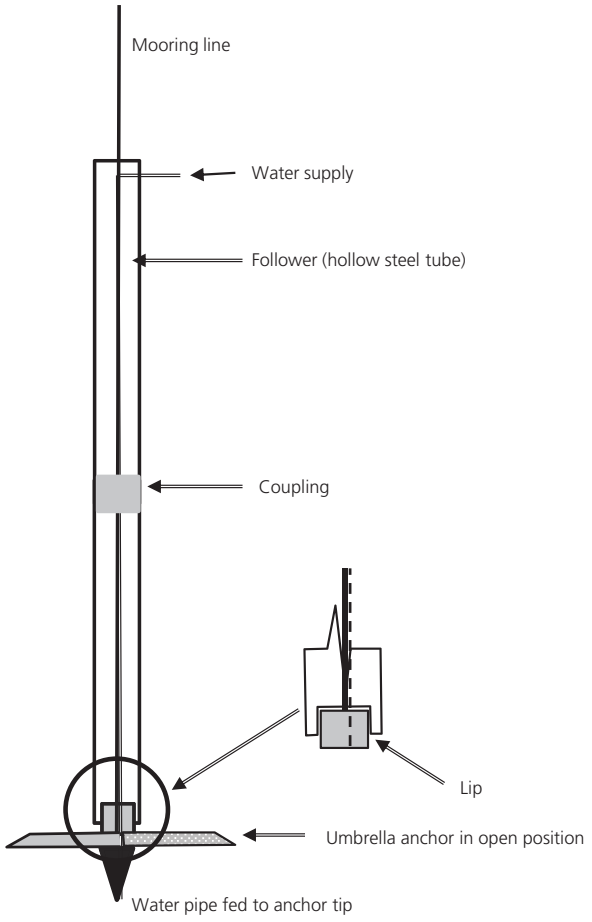

Figure 3. Follower with anchor attached

2.1 Analysing plate anchor behaviour in sand

The capacity of a buried plate anchor is dependent on the embedment depth, shape, orientation, loading type and loading angle (in-plane or out-of-plane) and the stiffness of the soil (Bradshaw *et al*., 2016). Murray and Geddes (1987) showed that the anchor pull-out capacity increased as the embedment ratio increased. Centrifuge studies on plate anchors by Ovesen (1981) and Dickin and Leung (1992) showed that the pull-out capacities provided by centrifuge modelling were much lower than similar tests carried out under normal gravity (1g). Tagaya *et al*. (1988) and Ilamparuthi *et al*. (2002) addressed the scaling issues associated with 1g model tests by using relatively large-scale plate anchors with diameters ranging between 100 and 400 mm.

2.2 Experimental programme

Nine tests were performed on anchors of two different sizes, inserted at different normalised embedment depths (H/D, where H is the anchor depth and D is the projected or equivalent dimension). In the presentation of the experimental data, two different 'equivalent' dimensions (D) were used. D_1 was equivalent to the width of the fully opened umbrella anchor (see Figure 4) and D_2 was taken as the diameter of a circular plate of the same total surface area as the four wings of the umbrella anchor. When normalising the anchor depth by D_1, the embedment ratios (H/D) of the tests were between 1.8 and 5.3; when using D_2 (based on an equivalent surface area), H/D values were between 2.2 and 6.2. To confirm the capacity and displacement behaviour of the fully opened anchors, tests were also carried out on 'wished-in-place' anchors (placed fully open in the sand bed), for both anchor sizes at the greatest depths of embedment (Table 1). These 'wished-in-place' tests were also used to verify whether or not the disturbance of the sand bed caused during installation had any noticeable effect on the pull-out behaviour.

2.3 Anchor geometry and testing chamber

The larger umbrella anchor, UA1, had a width D_1 of 334 mm and surface area of 58 000 mm^2 when fully opened, which equated to an equivalent diameter D_2, based on the surface area, of 272 mm (Figures 2 and 4). The smaller umbrella anchor, UA2, had a width D_1 of 223 mm and surface area of 29 000 mm^2 when fully opened, which equated to an equivalent diameter D_2 of 192 mm. The thickness of the plates was 10 mm in both UA1 and UA2. The smaller anchor was designed to project a surface area that was half that of the larger anchor. Stainless steel slings (8 mm dia.) with a capacity of 50 kN were used as mooring lines to connect the anchor to the load cell.

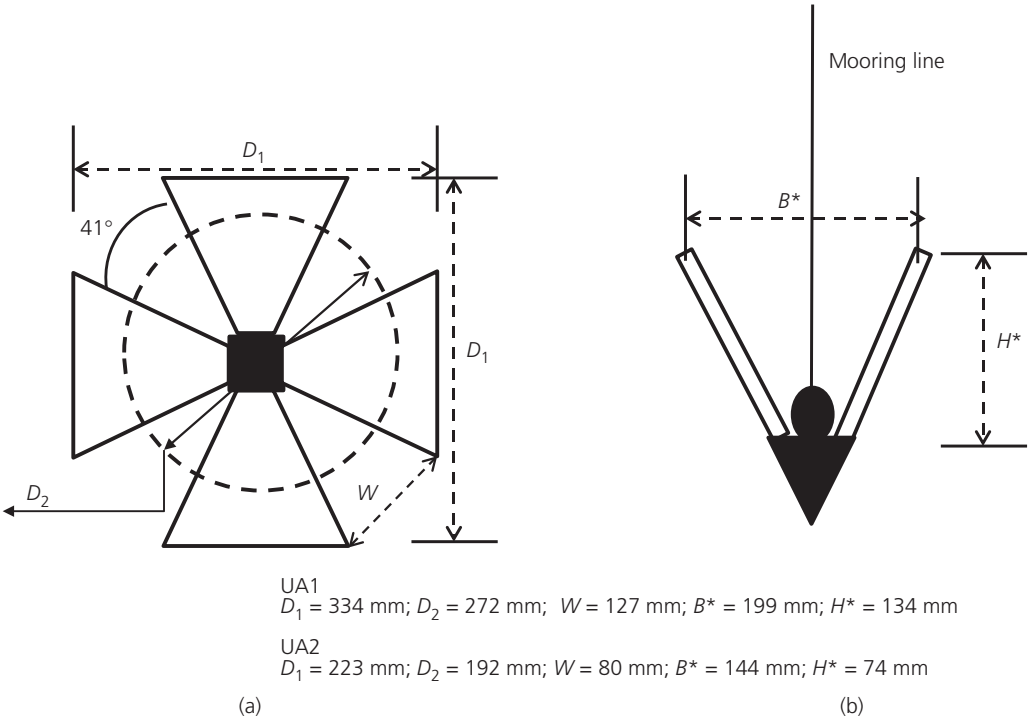

Figure 4. Umbrella anchors used in testing with dimensions: (a) plan view of opened anchor; (b) section of closed anchor

Table 1. Summary of testing schedule

Test number	Embedment ratio (H/D) where $D = B$	Embedment ratio (H/D) where D is based on the equivalent area	Test type	Anchor size
1	4.8	5.9	Wished-in-place	UA1
2	4.9	6.1	Installed and loaded	
3	3.9	4.8	Installed and loaded	
4	2.5	3.1	Installed and loaded	
5	1.8	2.2	Installed and loaded	
6	5.2	6.0	Wished-in-place	UA2
7	5.3	6.2	Installed and loaded	
8	4.2	4.9	Installed and loaded	
9	2.7	3.1	Installed and loaded	

A follower was used to push the anchor into place. It was made using two 800 mm long sections of hollow steel tube with an outer diameter of 64 mm and wall thickness of 5 mm. The two sections of this follower could be bolted together through a coupling, as shown in Figure 3. The lower half of the follower had a lip, which allowed the anchor to be secured in place during installation and prevented any rotation. The water supply line shown in Figure 3 was connected to an outdoor tap with a control on the outlet pressure. The vibrating force was applied at the top end of the follower, using the vibrating hammer.

Figure 5(a) shows the testing chamber containing the sand bed. This chamber was constructed using four concrete rings (internal diameter 1.2 m; height of each ring 0.5 m; thickness 0.08 m). The rings were sealed at the joints using cement paste. A frame was secured using steel square hollow sections and bolted to the top of the concrete rings. A 12 V electric car winch with a capacity of 50 kN was bolted to the frame. A snatch block was used to increase the load on the anchor by means of strain control at a rate of 2 mm/s. A 50 kN load cell was located in the mooring line and the winch hook, as shown in Figure 5, to measure the pull-out force. A cable-extension position transducer was used to measure the displacement of the anchor. The full experimental set-up is shown in Figure 5(b).

2.4 Soil bed preparation

The tests were carried out in beds of fine-to-medium sand which had particle sizes D_{10}, D_{30} and D_{60} of 0.2 mm, 0.25 mm and 0.35 mm, respectively (Table 2 and Figure 6). To form a saturated soil bed the lower section of the chamber was initially filled with

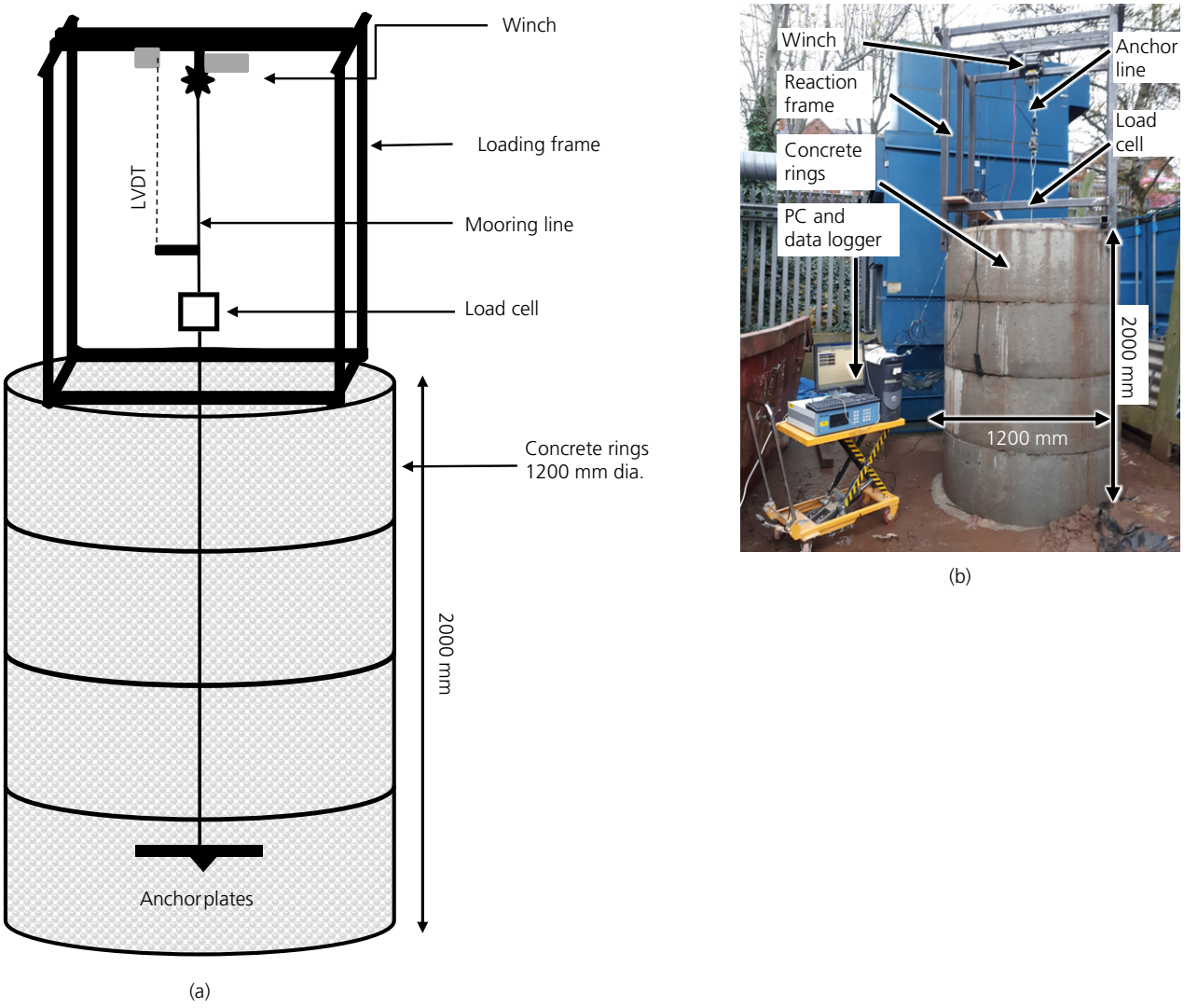

Figure 5. Testing chamber, loading frame and instrumentation: (a) line diagram; (b) digital image of the set-up. LVDT, linear variable displacement transducer

Table 2. Properties of soil

Classification parameters	Values
D_{60}; D_{30}; D_{10}	0.20; 0.25; 0.35 mm
C_u : C_g	1.7 : 0.8
Classification	Uniformly graded sand
Angle of internal friction (peak and ultimate)	40° and 37°
Angle of dilation	4°

water. Sand was then poured into the chamber in layers 300 mm thick, with light tamping applied to each layer, to improve the uniformity of the soil bed. Upon completion of the sand bed, the water level in the chamber was maintained 50 mm above the finished sand surface. For the wished-in-place tests, the anchor was placed fully opened at the required depth and the remainder of the sand bed was formed using the above procedure.

The peak and ultimate angles of internal friction of the sand were measured in a shear box under a vertical pressure of 15 kPa. This was the average vertical effective stress in the sand when the chamber was full. The peak and the ultimate friction angles were 40° and 37°, respectively. The dilation angle was 4° at the peak state.

A cone penetrometer was manufactured for this research at Queen's University Belfast, to establish the uniformity of the sand beds (Figure 7). The cone had a tip angle of 60° and surface area of 1500 mm^2. This cone was pushed into the soil bed at a slow rate (2 mm/s), and the force on the cone was measured using a load cell located above the cone, as illustrated in Figure 7. Before the installation of the anchor, cone penetrometer tests were carried out in the centre of the sand bed, as this area would be disturbed by the installation of the

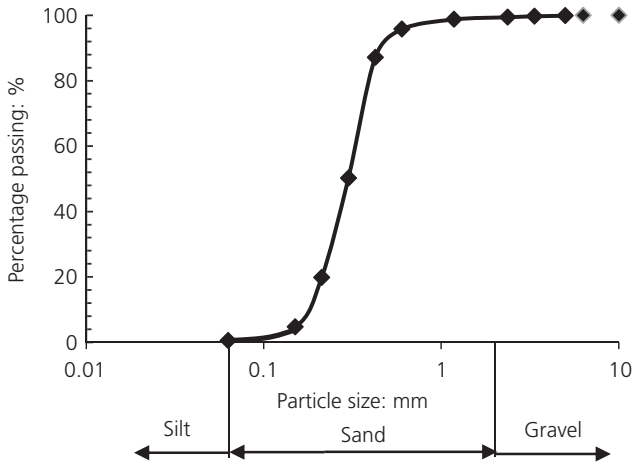

Figure 6. Particle size distribution of sands

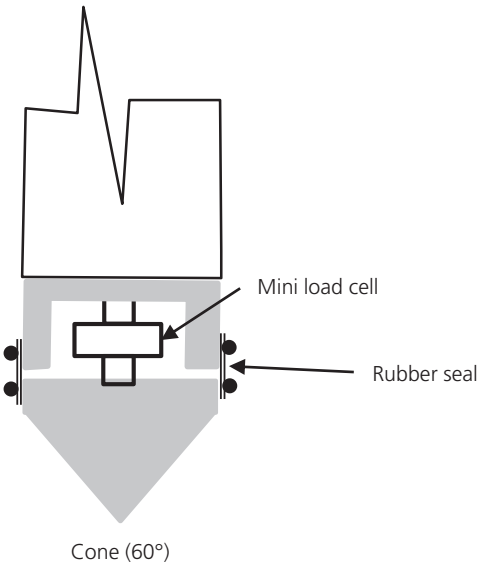

Figure 7. Diagram of cone penetrometer used in testing

anchor. For the wished-in-place anchor tests, the cone penetrometer tests were carried out before the pull-out tests at a point 300 mm from the chamber wall. The reason for this is to avoid any rotation of the anchor due to disturbances of the sand caused by installing and removing the cone penetrometer.

The profiles of cone tip resistance with depth for each test are shown in Figure 8. Owing to limitations of the test equipment, profiles could only be taken to a maximum depth of 1600 mm. The tip resistance linearly increased with depth. The consistency of the tip resistance among nine test beds was good and confirmed the uniformity of the soil beds. Using the measured tip resistance and the empirical model, as proposed by Kim *et al.* (2016), the relative density of the sample was estimated to range from 47% at a depth of 200 mm to 56% at 1600 mm.

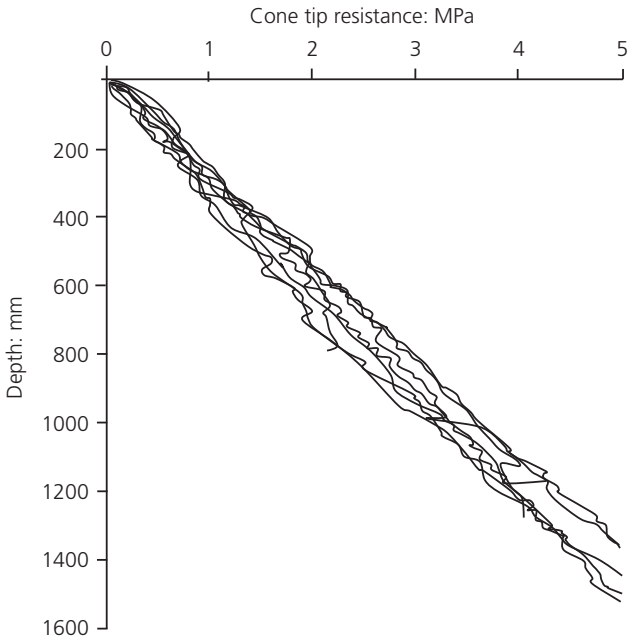

Figure 8. Cone penetration test profiles

After the anchor had been installed to a required depth, pull-out tests were performed. The vertical displacement, H^* (Figure 4), required for the anchor wings to open fully is approximately 134 mm in the case of UA1 and 74 mm in the case of UA2. These displacements are based on the geometry presented in Figure 4. However, the actual vertical displacement required for the wings to open could be higher than these values due to small deformation of the soil above the wings during initial pull-out. The wished-in-place anchors were located at slightly lower embedment depths than the dynamically installed anchors (by 134 mm for UA1 and 74 mm for UA2) so that the H/D ratios after full opening of the wings would be approximately the same for both installation methods.

The follower was removed upon reaching the required depth and the mooring line was then attached to the winch and subjected to a small amount of tension. Figure 9 shows images of the unearthed anchors. Figure 9(a) shows the top end of the closed anchor, after installation, but without a pull-out load applied to the anchor. Figure 9(b) was taken after a test had been completed and the anchor unearthed. This confirmed that the anchor wings had fully opened with the application of a pull-out load.

2.5 Predictive models

The space between the fully opened wings (W in Figure 4) ranged from 15 to 127 mm for UA1 and 15 to 80 mm for UA2. The angle between the wings was approximately 41°. Owing to the small size of these gaps, the failure zones of each anchor wing would interact with each other upon pull-out.

(a) (b)

Figure 9. Photographs of the unearthed anchor: (a) closed after installation; (b) fully opened after pull-out

The combined zone above the anchor wings could fail as one overlapping or composite mechanism, as opposed to four separate failure zones. This behaviour of interfering anchor plates has been examined in the past by Geddes and Murray (1995) and Kumar and Kouzer (2008). It also highlights a need for simplification in assuming equivalent circular plate anchors for the analysis of the umbrella anchor behaviour. This assumption is appraised and expanded upon further in the following sections.

Plots of pull-out capacity for plate anchors are frequently presented in terms of breakout factors, N_q, and this approach is adopted here. The measured pull-out forces were converted to breakout factors using the following equation.

1. $$N_q = \frac{q_u}{\gamma' H}$$

where q_u is the pull-out forced divided by the anchor area; γ' is the effective unit weight of the sand; and H is the depth of the anchor below the soil surface. To appraise the effect of the gaps between the opened wings, while not knowing the exact failure mechanism, the measured pull-out capacities of each anchor were plotted as two different breakout factors using the corrected diameters, D_1 and D_2, as described earlier. Analytical methods for shallow circular plate anchors presented by Murray and Geddes (1987) and Ilamparuthi *et al.* (2002) were used to predict the anchor capacity achieved by the umbrella anchors. It is recognised that other methods are available in the literature; however, for this feasibility study the above methods were adopted because of their simplicity.

Murray and Geddes (1987) proposed an upper bound plasticity solution adopting an associated flow rule (where the angle of dilation equals the angle of friction) to predict N_q:

2. $$N_q = 1 + 2\frac{H}{D}\tan\Phi'\left(\frac{2}{3}\frac{H}{D}\tan\Phi' + 1\right)$$

while Ilamparuthi *et al.* (2002) proposed a series of empirical equations (Equations 3–9):

3. $$N_{qf} = e^{(33.5/28)(H/D)} \text{ for } 0.0 \leq H/D \leq 1.0$$

4. $$N_{qf} = (H/D)N_{qf1} \text{ for } 1.0 < H/D \leq 2.4$$

5. $$N_{qf} = (H/2D)(e^{\tan\Phi \times \ln(H/D)})N_{qf1} \text{ for } 2.4 < H/D \leq 4.2$$

6. $$N_{qf} = [(H/D) + (H/D)(e^{\tan\Phi \times \ln(D/H)})]N_{qf1} \text{ for } 4.2 < H/D \leq 6.0$$

7. $$N_{qf} = [(H/D) + (e^{\tan\Phi \times \ln(H/D)})]N_{qf1} \text{ for } 6.0 < H/D \leq 10.0$$

8. $$N_{qf} = [N_{qf10} + e^{\tan\Phi \times \ln(H/D\ -\ 10)}] \text{ for } 10.0 < H/D \leq 12.0$$

9. $$N_{qf}^{\Phi} = N_{qf}^{33.5}[e^{(H/3D)(\Phi - 33.5)/33.5}]$$

where Φ' is the friction angle.

In these equations, N_{qf} is the breakout factor for an anchor in loose sand with $\Phi' = 33.5°$ and N_{qf1} and N_{qf10} are the breakout factors for $H/D = 1.0$ and 10.0, respectively. Equation 9 can be used to predict a breakout factor N_{qf}^{Φ} for any embedment ratio and friction angle for denser sands. Ilamparuthi *et al.* (2002)

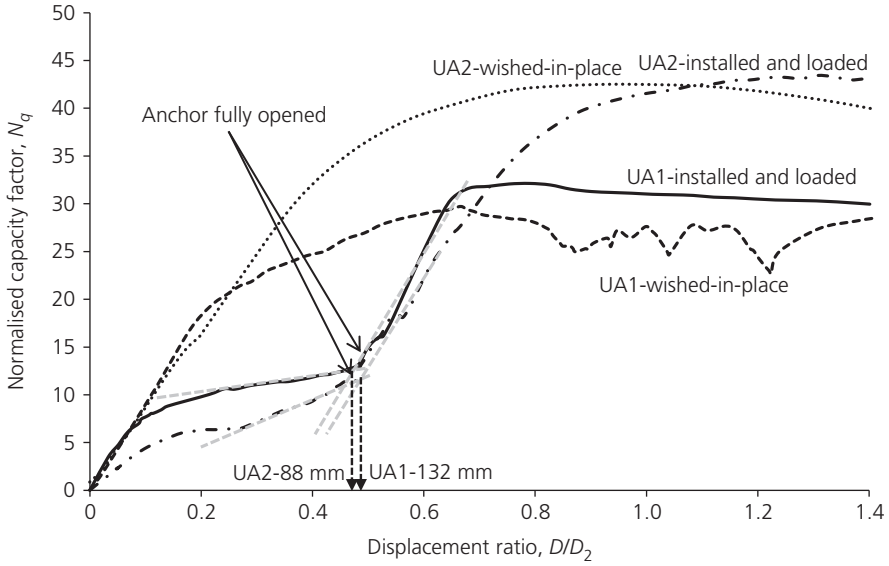

Figure 10. Wished-in-place and installed and loaded test comparison for both anchors, with labels indicating the point at which the anchor had opened fully

postulated that transitional behaviour (i.e. shallow failure to deep failure) occurred at embedment ratios varying from 4.8 to 6.8 depending on the density of the sand.

3. Results

3.1 Anchor capacity

Figure 10 shows a comparison of the breakout factor, N_q, plotted against the anchor displacement, δ, normalised by D_2 for wished-in-place and dynamically installed anchors with H/D of about 6.0. This made it possible to establish whether or not the wings of the dynamically installed anchors opened up at the predetermined vertical displacement based on the geometry of the anchors. To assess this, simple graphical constructions (dashed grey lines in Figure 10) were carried out to estimate the vertical displacements at which the wings fully opened. Approximate values of vertical displacement are 132 mm and 82 mm for UA1 and UA2, respectively. These displacements are in close agreement with the theoretical values based on the geometry of the anchors (H^*, Figure 4).

For the wished-in-place tests, the pull-out forces on the anchors steadily increased to a maximum pull-out capacity, N_q, of 30 and 41 for UA1 and UA2, respectively. However, the dynamically installed anchors showed slightly different responses. N_q increased slowly to a value of approximately 10 at a normalised displacement of 0.48, which corresponds to displacements of 127 mm and 92 mm for UA1 and UA2, respectively. These displacements are approximately equal to the vertical height H^* of the anchor wings when fully closed (Figure 4). The breakout factor for UA1 and UA2 was 32 and 42 at normalised displacement of approximately 0.7 and 1.2, respectively. The capacity of the dynamically installed and wished-in-place anchors are in close agreement. This also suggests minimal soil disturbances during the installation of anchors.

Figures 11 and 12 show the effect of H/D on the normalised load–displacement plots for all tests performed for UA1 and UA2, respectively. Observations show the occurrence of a step in the load, as the anchor wings deployed, followed by an increase in load and a peak resistance similar to the wished-in-place tests. To open fully, both anchor sizes required a vertical displacement of about $0.5D_2$ (diameter of the equivalent circle) or $0.4D_1$ (width of the fully opened anchor), as shown in Figures 11 and 12. The load–displacement plots give no indication that the embedment depth influenced this opening distance. The observations showed a peak in anchor capacity, which then decreased, due to the reduction in confining and overburden pressures as the anchor moved upwards.

The peak pull-out capacity factors achieved at different embedment ratios for UA1 (anchor having D_1 of 334 mm) are shown in Figure 13. This figure also shows the predicted pull-out capacities calculated from existing analytical tools, assuming the peak angle of internal friction of 40°. The observed breakout factors show that pull-out capacity increases with embedment ratio, as expected. When the actual area of the anchor is used to determine the pull-out capacity factors (i.e. the area based on the equivalent diameter D_2), the observed capacity is close to that predicted by Murray and Geddes (1987) and Ilamparuthi *et al*. (2002) up to an embedment ratio of around 4.8. The tests carried out at embedment ratios greater than 4.8 provided capacities that were lower than expected. As discussed earlier, embedment ratios of 4.8 and 6.8 are typical values for

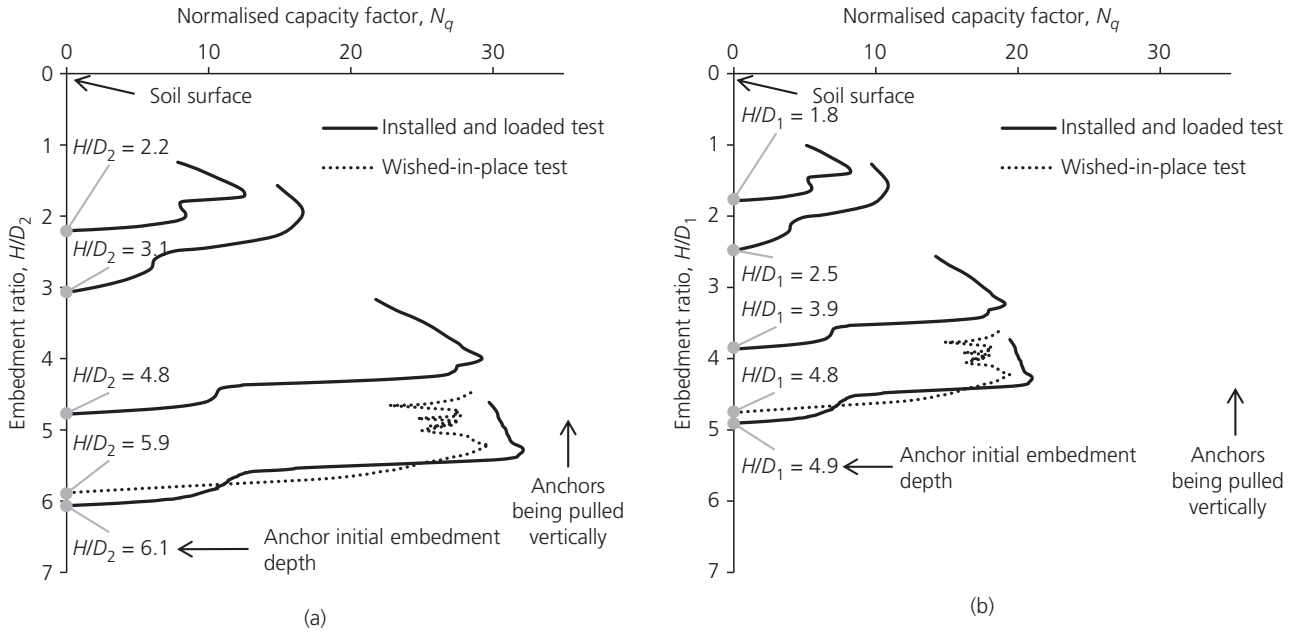

Figure 11. Normalised load–displacement plots for all UA1 (larger anchor) tests: (a) normalised using equivalent diameter and actual anchor area; (b) normalised using width of fully opened anchor and projected area

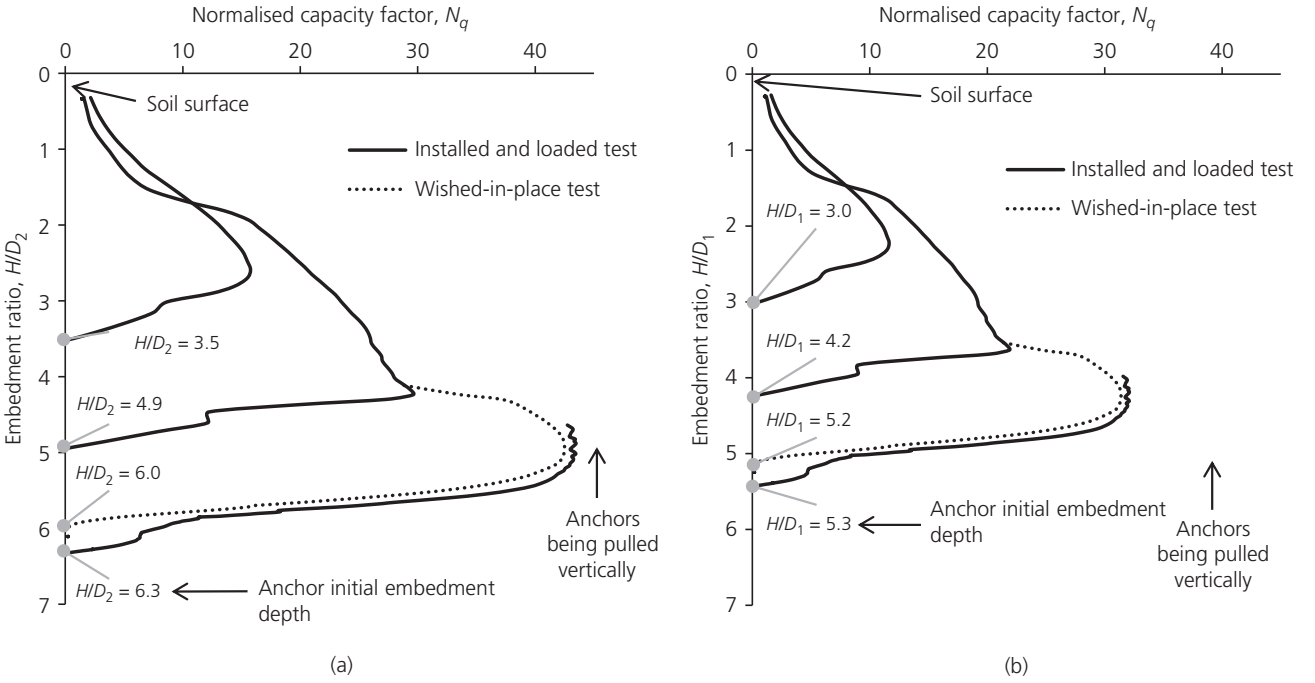

Figure 12. Normalised load–displacement plots for all UA2 (smaller anchor) tests: (a) normalised using equivalent diameter and actual anchor area; (b) normalised using width of fully opened anchor and projected area

the transition behaviour from a shallow to a deep failure mechanism in loose and dense sand, respectively (Ilamparuthi *et al*., 2002; Meyerhof and Adams, 1968). It should also be noted that the transition limits are dependent on anchor shape and size, as well as boundary conditions. The case presented in the present investigation is not typical as there were four irregularly shaped wings, but they all connected by way of the same pull-out unit. The sand bed used in the investigation was loose

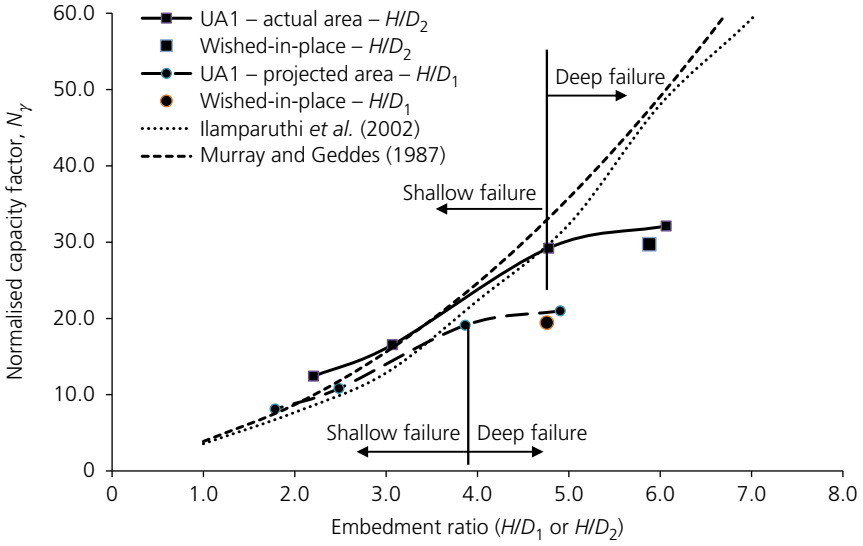

Figure 13. Normalised peak capacity for UA1 and analytical models

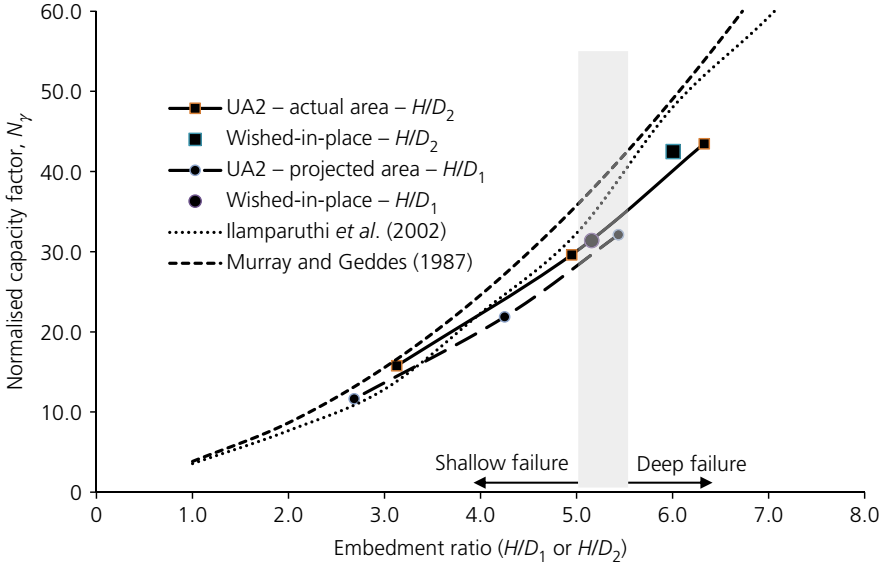

Figure 14. Normalised peak capacity for UA2 and analytical models

to moderately dense. Assuming the model predictions reported by Murray and Geddes (1987) and Ilamparuthi *et al.* (2002) are reasonable estimates for the pull-out capacities, it could be expected that the transition behaviour was at an H/D ratio of 4.8 and this was the case when the data were analysed based on equivalent diameter D_2. However, for an H/D ratio based on the actual width of the anchor, the transition behaviour took place at an H/D ratio of about 3.9 (Figure 13), which may not be realistic. In essence, it is difficult to assign an 'equivalent diameter' to an anchor unit with a complex shape. Nevertheless, it appears that a deep failure mechanism may have occurred in UA1 at an H/D ratio lower than might be expected in loose to medium sand. Such behaviour can be attributed to possible boundary effects caused by the concrete cylinder, the diameter of which was only 3.6 times more than the width of the anchor. However, a minimum ratio of 5 is generally required to avoid boundary effects (Bolton and Gui, 1993; Palmeira and Milligan, 1989; Ullah *et al.*, 2017).

Figure 14 shows the normalised capacity for UA2 – the smaller anchor – at varying embedment ratios along with the predicted capacities. When the anchor capacity and

embedment ratio were normalised using the actual anchor area and equivalent diameter, the observed capacity was close to that predicted by Murray and Geddes (1987) and Ilamparuthi *et al*. (2002). It should be noted that the predicted results exceed the measurements beyond an embedment ratio of 5.0. When the anchor's projected area and full width D_1 are used to normalise the results in the UA2 tests, the capacity achieved is generally less than the predicted values. The notably reduced increase in anchor capacity observed at the greatest embedment ratios for the UA1 test did not occur for UA2, which was earlier attributed to a possible boundary effect, triggering a premature deep failure mechanism. In UA2, boundary effects are significantly less because the size of the anchor (based on width) is 5.4-fold smaller than the diameter of the concrete cylinder housing the sand.

4. Discussion

4.1 Potential field application

The initial application of the anchor was assessed in granular soils such as fine-to-medium sand. Since the installation procedure heavily relies upon 'liquefaction effects', the proposed anchor mechanism is only suitable to be used in silt and up to medium sand. It will not be effective in coarse sand and gravel. However, it can also be used in clay deposits with a soft to firm consistency. The anchor installation procedure, using a simple vibrating mechanism and water jetting facility, proved successful, as installation of the anchor to a depth of 1.6 m could be readily achieved in minutes, by a single operator. It was found that as the anchor penetrated further into the sand bed the required installation effort reduced significantly. This could be due to excess pore pressure being generated by the vibrations (liquefaction effects) and insufficient time for it to dissipate due to a long drainage path, although the sand bed was highly permeable. In the case of the sand deposit, cavity formation behind the anchor during installation was not found to be an issue.

There are two other concerns in the current form of anchor design: (*a*) a significant bending moments and shear stresses can occur at the points where the anchor plates are supported and (*b*) there is a possibility of buckling of the follower. The structural stability of the umbrella anchor in practical applications is of paramount importance. Notably, bending stresses in the wings under operational conditions can be assessed from the bearing capacity calculations and the likely eccentricity of the loadings. Other potential structural issues are: pin failure under shear and bearing failure under the supporting protrusion (Figure 1). A complete structural analysis is therefore necessary prior to a potential investigation of a protype anchor system. However, preliminary calculations have shown that (for the configurations used in this investigation) the shear loading on each of the supporting protrusions and pins in UA1 at the deepest embedment ratio can be as high as 5.0 kN with about 0.56 kNm of bending moment on the plate. The most obvious failure of the system could be associated with the pins. The pins (dia. 8 mm) were made of mild steel and, based on the yield stresses, under the current loading conditions the factor of safety against shear failure was approximately 7.0. The shear loading and the bending moment can be reduced significantly by having chain links between the wings and the extended central shaft, as shown in Figure 15. Such an addition to the proposed anchor system will not interfere with the installation process as the chains will be contained within the folded wings.

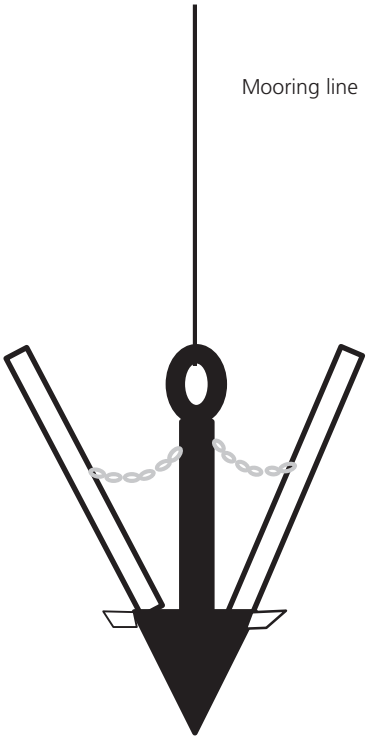

Figure 15. Possible alteration to anchor system

4.2 Pull-out capacity

The behavioural trends of the bearing capacity factors for both anchor sizes were generally reasonably consistent with the trends predicted by Murray and Geddes (1987) and Ilamparuthi *et al*. (2002). There were, however, disparities between the predicted behaviour and the actual behaviour at the greatest depth of embedment for test series UA1 for the larger anchor. The authors believe that the anchor at this depth behaved as a deep anchor, thus the current models do not reflect the actual behaviour of the subsoil. The predictions also tend to exceed the experimental evidence of the UA2 smaller anchor test series at large depths. This is not wholly surprising, as the analytical approach of Murray and Geddes (1987) should provide an upper bound solution.

It is suggested that the overlapping failure mechanism of the individual anchor wings caused the sand above the anchor to fail as

one complex mechanism, and there appears to be some justification for developing an analysis based on equivalent circular plate anchors, although further research is needed to investigate the concept fully. There are a number of other factors that need investigating in developing the system. These include: the effects of anchor inclination and loading angle; the effects of repeated cyclic loading on pull-out capacity; and suction effects behind the anchor, particularly under rapid dynamic loading. Other factors of interest are: possible liquefaction in front of the anchor due to vibrations and oscillations in loading; exploration of the behaviour in fine subsoils; and extending the predictive analyses for shallow and deep anchors to full-scale prototype anchors.

5. Scale effects

Although no specific prototype size was specified, it is anticipated that the ratio of model to prototype scale could be on the order of 1:5. The present physical modelling involved two steps: (*a*) installation of the anchor by a combination of jetting at the anchor tip to liquefy the soil along with vibratory driving; (*b*) application of pull-out loads to the anchor after installation. Scale effects associated with anchor pull-out can be more easily addressed. However, the major limitation of reduced-scale 1***g*** testing is that the stresses in the soil do not scale with geometry, which can affect the soil constitutive response. It is expected that monotonic loading of the model anchor occurred under drained conditions. If the model soil is prepared to the same relative density as the prototype, the model soil will have higher dilation and strength due to the lower confining pressures. The loads and displacements will also be lower in the model. Previous 1***g*** studies on plate anchors and foundations (e.g. Bradshaw *et al.*, 2016; Kelly *et al.*, 2006; LeBlanc *et al.*, 2010) have addressed these effects by: (*a*) presenting the load test results in terms of non-dimensional quantities; (*b*) preparing the soil looser in the model than in the prototype, such that the soil has the same dilation response and peak friction angle. The soil friction angle in the physical model in this study was estimated to be 40° based on element tests performed at comparable void ratios and confining pressures. Cone testing suggested that the soil had a relative density of around 50%. Therefore, the dimensionless model test results should be representative of a prototype anchor embedded in sand with a friction angle of 40°. Since the confining pressures in the prototype will be higher, and thus more contractive, the relative density in the prototype would be higher, on the order of 65% for a scale factor of 5 for example, to achieve the same dilatancy index (Bradshaw *et al.*, 2016).

6. Conclusions

This paper has reported data from an initial development stage of an 'umbrella anchor' concept, where the anchor was pushed into a sand deposit in a folded arrangement to reduce installation loads, and it opened up upon applying a pull-out load to generate a large bearing area. The investigations were carried out in a large concrete chamber housing fine sand placed in a loose to moderately dense state. The installation methods (in the form of vibration and liquefaction) adopted in the investigations were found to be straightforward and can be adopted in full-scale application. The following are the key conclusions from the investigations.

- Upon the application of a vertical pull-out load, the anchor deployed a large, embedded plate area. The wings opened up at the pre-determined vertical displacements based on the geometry of the anchors. The vertical displacement required for this was approximately $0.5D_2$ (where D_2 is the equivalent diameter). Opening of the wings was further verified by unearthing the anchor after peak pull-out capacity had been achieved.
- The vertical displacement required to fully open the anchors did not appear to be dependent on the embedment depth but was a function of the anchor geometry.
- The pull-out capacities of the dynamically installed and wished-in-place anchors are in close agreement.
- The predicted pull-out capacity factors using existing analytical tools are in good agreement with the observed performance when the equivalent diameter D_2 is used for the determination of pull-out capacity.
- Transition behaviour from shallow failure to deep failure took place at slightly lower values of H/D ratios for UA1. However, this could be attributed to possible boundary effects caused by the concrete cylinder housing the sand bed. It appears, as noted in the existing literature, that the transition behaviour from shallow to deep failure in the case of UA2 took place at high values of H/D ratios.
- The proposed anchor configuration requires modifications in order to avoid any potential mechanical failure, in particular at the hinge connecting the plates to the pull-out unit.

Acknowledgement

The funding for the project was provided by the Department for Learning and Employment, NI, UK under the US–Ireland R&D partnership (grant no. USI-041).

REFERENCES

Aubeny C (2019) *Geomechanics of Marine Anchors*, 1st edn. CRC Press, Boca Raton, FL, USA.

Bolton MD and Gui MW (1993) *The Study of Relative Density and Boundary Effects for Cone Penetration Tests in Centrifuge.* Engineering Department, Cambridge University, Cambridge, UK, CUED/D-SOILS/TR256.

Bradshaw AS, Giampa JR, Gerkus H *et al.* (2016) Scaling considerations for 1-g model horizontal plate anchor tests in sand. *Geotechnical Testing Journal* **39(6)**: 1006–1014.

Byrne BW and Houlsby GT (2015) Helical piles: an innovative foundation design option for offshore wind turbines. *Philosophical Transactions: Mathematical, Physical and Engineering Sciences* **373(2035)**: 20140081, https://doi.org/10.1098/rsta.2014.0081.

Chang K, Hossain SM, Wang D and Kim HY (2019) Performance of a novel dynamically installed fish anchor in calcareous silt. *Journal of Geotechnical and Geoenvironmental Engineering* **145(6)**: 04019019.

Das BM and Seeley GR (1975) Breakout resistance of shallow horizontal anchors. *Journal of the Geotechnical Engineering Division* **101(GT9)**: 999–1003.

Dickin EA and Leung CF (1992) Influence of foundation geometry on the uplift behaviour of piles with enlarged bases. *Canadian Geotechnical Journal* **29(3)**: 498–505, https://doi.org/10.1139/t92-054.

Frankenmolen S, Erbrich CT and Fearon R (2017) Successful installation of large suction caissons and driven piles in carbonate soils. In *Proceedings of 8th International Conference on Offshore Site Investigation and Geotechnics*. Society for Underwater Technology, London, UK, pp. 539–548, https://doi.org/10.3723/OSIG17.539.

Gavin K, Igoe D and Doherty P (2011) Piles for offshore wind turbines: a state-of-the-art review. *Proceedings of the Institution of Civil Engineers – Geotechnical Engineering* **164(4)**: 245–256, https://doi.org/10.1680/geng.2011.164.4.245.

Geddes JD and Murray EJ (1995) Plate anchor groups pulled vertically in sand. *Journal of Geotechnical Engineering* **122(7)**: 509–516, https://doi.org/10.1061/(ASCE)0733-9410(1996)122:7(509).

Giampa JR, Bradshaw AS and Schneider JA (2017) Influence of dilation angle on drained shallow circular anchor uplift capacity. *International Journal of Geomechanics* **17(2)**: 04016056, https://doi.org/10.1061/(ASCE)GM.1943-5622.0000725.

Giampa J, Bradshaw A, Gerhus H *et al.* (2019) The effect of shape on the pull-out capacity of shallow plate anchors in sand. *Géotechnique* **69(4)**: 355–363, https://doi.org/10.1680/jgeot.17.P.269.

Hossain SM, Mohiuddin MA, Dalal A and Turner BS (2023) Field performance of the fish anchor. *Journal of Geotechnical and Geoenvironmental Engineering* **149(2)**: 06022014, https://doi.org/10.1061/JGGEFK.GTENG-10437.

Houlsby GT and Byrne BW (2005) UK design procedures for installation of suction caissons in clay and other materials. *Proceedings of the Institution of Civil Engineers – Geotechnical Engineering* **158(2)**: 75–82, https://doi.org/10.1680/geng.2005.158.2.75.

Ilamparuthi K, Dickin EA and Muthukrisnaiah K (2002) Experimental investigation of the uplift behaviour of circular plate anchors embedded in sand. *Canadian Geotechnical Journal* **39(3)**: 648–664.

Jalilvand S, Gavin KG, Sivakumar V, Gilbert R and Bradshaw B (2022) New insights into the failure mechanisms of horizontal plate anchors in clay during pull-out. *Géotechnique* **72(3)**: 189–199, https://doi.org/10.1680/jgeot.18.P.283.

Kelly RB, Houlsby GT and Byrne BW (2006) A comparison of field and laboratory tests of caisson foundations in sand and clay. *Géotechnique* **56(9)**: 617–626, https://doi.org/10.1680/geot.2006.56.9.617.

Kim YH and Hossain MS (2017) Dynamic installation, keying and diving of OMNI-Max anchors in clay. *Géotechnique* **67(1)**: 78–85, https://doi.org/10.1680/jgeot.16.T.008.

Kim JH, Choo YW and Kim DJ (2016) Miniature cone tip resistance on sand in a centrifuge. *Journal of Geotechnical and Geoenvironmental Engineering* **149(3)**: 04015090, https://doi.org/10.1061/(ASCE)GT.1943-5606.0001425.

Kumar J and Kouzer KM (2008) Vertical uplift capacity of a group of shallow horizontal anchors in sand. *Géotechnique* **58(10)**: 821–823, https://doi.org/10.1680/geot.2008.58.10.821.

Lai Y, Zhu B, Huang Y and Chen C (2020) Behaviour of drag embedment anchor in layered clay profiles. *Applied Ocean Research* **101**: 102287.

LeBlanc C, Houlsby GT and Byrne BW (2010) Response of stiff piles in sand to long-term cyclic lateral loading. *Géotechnique* **60(2)**: 79–90, https://doi.org/10.1680/geot.7.00196.

Lee J and Aubeny CP (2020) Multiline ring anchor system for floating offshore wind turbine. *Journal of Physics: Conference Series* **1452(2020)**: 012036.

Lee J, Balakrishnan K, Aubeny CP *et al.* (2021) Uplift resistance of a multiline ring anchor in soft clay to extreme conditions. In *Geo-Extreme 2021* (Meehan CL, Pando MA, Leshchinsky BA and Jafari NH (eds)). American Society of Civil Engineers, Reston, VA, USA, Geotechnical Special Publication no. 328, pp. 413–424.

Liu H, Li Y, Yang H, Zhang W and Liu C (2010) Analytical study on the ultimate embedment depth of drag anchors. *Ocean Engineering* **37(14–15)**: 1292–1306.

Liu H, Liu C, Yang H *et al.* (2012) A novel kinematic model for drag anchors in seabed soils. *Ocean Engineering* **49**: 33–42.

Meyerhof GG and Adams JL (1968) The ultimate uplift capacity of foundations. *Canadian Geotechnical Journal* **5(4)**: 2225–2244.

Murray EJ and Geddes JD (1987) Uplift of anchor plates in sand. *Journal of Geotechnical Engineering* **113(3)**: 202–215.

Neubecker SR and Randolph MF (1996) The static equilibrium of drag anchors in sand. *Canadian Geotechnical Journal* **33(4)**: 574–583.

O'Loughlin CD, Blake AP, Richardson MD, Randolph MF and Gaudin C (2014) Installation and capacity of dynamically embedded plate anchors as assessed through centrifuge tests. *Ocean Engineering* **88**: 204–213.

O'Neill MP, Bransby MF and Randolph MF (2003) Drag anchor fluke–soil interaction in clays. *Canadian Geotechnical Journal* **40(1)**: 78–94.

Ovesen NK (1981) Centrifuge tests on the uplift capacity of anchors. *Proceedings of the 10th International Conference on International Society for Soil Mechanics and Geotechnical Engineering (ISSMGE), Stockholm, Sweden*, vol. 1, pp. 717–722.

Palmeira EM and Milligan GWE (1989) Scale and other factors affecting the results of pull-out tests of grids buried in sand. *Géotechnique* **39(3)**: 511–524, https://doi.org/10.1680/geot.1989.39.3.511.

Randolph M, Gourvenec S, White D and Cassidy M (2011) *Offshore Geotechnical Engineering*. Spon Press, Abingdon, UK.

Richardson BE (2008) *Dynamically Installed Anchors for Floating Offshore Structures*. PhD thesis, The University of Western Australia, Perth, Australia.

Roy A, Chow SH, O'Loughlin CD, Randolph MF and Whyte S (2021a) Use of a bounding surface model in predicting element tests and capacity in boundary value problems. *Canadian Geotechnical Journal* **58(6)**: 782–799, https://doi.org/10.1139/cgj-2019-0841.

Roy A, Chow SH, O'Loughlin CD and Randolph MF (2021b) Towards a simple and reliable method for calculating uplift capacity of plate anchors in sand. *Canadian Geotechnical Journal* **58(9)**: 1314–1333.

Sahoo JP and Ganesh R (2018) Vertical uplift resistance of rectangular plate anchors in two layered sand. *Ocean Engineering* **150**: 167–175.

Smith JE (1963) *Umbrella-Pile-Anchors*. U.S. Naval Civil Engineering Laboratory, Port Hueneme, CA, USA.

Tagaya K, Scott RF and Aboshi H (1988) Scale effect in anchor pull-outtest by centrifugal technique. *Soils and Foundations* **28(3)**: 1–12.

Thorne CP (1998) Penetration and load capacity of marine drag anchors in soft clay. *Journal of Geotechnical and Geoenvironmental Engineering* **124(10)**: 945–953.

Ullah SN, Hu Y, Stanier S and White D (2017) Lateral boundary effects in centrifuge foundation tests. *International Journal of Physical Modelling in Geotechnics* **17(3)**: 144–160.

Ullah SN, O'Loughlin C, Hu Y and Hou LF (2023) Torsional installation and vertical tensile capacity of helical piles in clay. *Géotechnique*, https://doi.org/10.1680/jgeot.22.00014.

Vesic AS (1971) Breakout resistance of objects embedded in ocean bottom. *Journal of the Soil Mechanics and Foundations Division* **97(9)**: 1183–1205.

Yu L, Zhou Q and Liu J (2015) Experimental study on the stability of plate anchors in clay under cyclic loading. *Theoretical and Applied Mechanics Letters* **5(2)**: 93–96.

Zhuang PZ, Yue HY, Song XG *et al.* (2022) Pull-out behaviour of inclined shallow plate anchors in sand. *Canadian Geotechnical Journal* **59(2)**: 239–253, https://doi.org/10.1139/cgj-2020-0495.

Zook JR and Keith AL (2009) Improvements in efficiency for subsea operations in deepwater Angola. *Proceedings of the SPE/IADC Drilling Conference and Exhibition, Amsterdam, the Netherlands*, SPE-119651-MS, https://doi.org/10.2118/119651-MS.